Proc. Natl. Acad. Sci. USA
Vol. 89, pp. 942–946, February 1992
Genetics

Structural analysis of a carcinogen-induced genomic rearrangement event

FREDERIC G. BARR*†‡, RICHARD J. DAVIS*, LAWRENCE EICHENFIELD*§¶, AND BEVERLY S. EMANUEL*‖**

*Division of Human Genetics and Molecular Biology, Children's Hospital of Philadelphia, Philadelphia, PA 19104; Departments of †Pathology and Laboratory Medicine and §Dermatology, Hospital of the University of Pennsylvania, Philadelphia, PA 19104; and Departments of ‖Pediatrics and **Human Genetics, University of Pennsylvania, Philadelphia, PA 19104

Communicated by Peter C. Nowell, October 7, 1991

ABSTRACT **We have explored the mechanism of genomic rearrangement in a hamster fibroblast cell culture system in which rearrangements are induced 5′ to the endogenous thymidine kinase gene by chemical carcinogen treatment. The wild-type region around one rearrangement breakpoint was cloned and sequenced. With this sequence information, the carcinogen-induced rearrangement was cloned from the corresponding rearranged cell line by the inverse polymerase chain reaction. After the breakpoint fragment was sequenced, the wild-type rearrangement partner (RP15) was isolated by a second inverse polymerase chain reaction of unrearranged DNA. Comparison of the sequence of the rearrangement breakpoint with the wild-type RP15 and 5′ thymidine kinase gene regions revealed short repeats directly at the breakpoint, as well as nearby A+T-rich regions in each rearrangement partner. Pulsed-field electrophoresis analysis demonstrated that this rearrangement is an interstitial deletion of 35 kilobases. Southern blot analysis of the RP15 region in unrearranged parental cells showed a demethylated CpG island and a complex of DNase I-hypersensitive sites adjacent to the breakpoint in the region deleted by the rearrangement. Therefore, these studies reveal interesting sequence and chromatin features near the rearrangement breakpoints and suggest a role for nuclear organization in the mechanism of carcinogen-induced genomic rearrangement.**

Numerous sporadic rearrangements have been identified in mammalian cells, both as acquired changes in tumors and as constitutional changes in heritable diseases. Characterization of the sequences at and near the breakpoints has provided evidence of multiple mechanisms of genomic rearrangement. Postulated mechanisms include mistakes in V(D)J recombination (1), homologous recombination between repetitive sequences (2), and nonhomologous recombination between regions with only 1- to 7-nucleotide blocks of junctional homology (3). Sequences capable of forming non-B-DNA structures, such as A+T-rich regions (4), homopurine and homopyrimidine tracts (5), and stretches of alternating purines and pyrimidines (6), as well as nuclear matrix attachment sites (7), have been identified near several rearrangement breakpoints and are postulated to disrupt chromatin structure and enhance accessibility for recombination.

Though sequence analysis of rearranged cell lines has yielded interesting clues, these systems are inherently limited. Since the rearrangement event occurred long before the cell line was derived, the nuclear organization of the parental cell type and the environmental conditions associated with the event are unknown. A better system for analyzing the mechanism of genomic rearrangement would be an inducible system in which a uniform cell population is exposed to an environmental perturbation resulting in a detectable rearrangement frequency at a locus of interest. A system in which the quiescent endogenous thymidine kinase (TK) gene of RJK92 Chinese hamster cells can be activated and rearranged following chemical carcinogen exposure has been developed (8, 9). Quantitative cell culture experiments and analysis of spontaneous TK^+ derivatives have indicated that carcinogen action induces the genomic rearrangements (9). We have adapted inverse polymerase chain reaction (PCR) methodology, which facilitates amplification of an unknown region flanking a known region (10, 11), for isolation of rearrangement breakpoints and the corresponding wild-type rearrangement partners. Inverse PCR involves cleavage on each side of the junction, circularization of the junctional fragment, and amplification with primers derived from the known sequence on one side of the junction. These amplified sequences were then utilized to investigate in the parental cell line the sequence, methylation status, and chromatin structure of the regions disrupted by one carcinogen-induced rearrangement event.††

METHODS AND MATERIALS

Cell Culture and DNA Isolation. Line 15 is an aminopterin-resistant TK^+ clone isolated following *N*-methyl-*N*′-nitro-*N*-nitrosoguanidine treatment of the aminopterin-sensitive TK^- Chinese hamster fibroblast cell line RJK92 (9). The hamster cell lines (line 15, RJK92, and TK^+ V79) were grown as described (9). For conventional gel electrophoresis and inverse PCR template construction, genomic DNA was isolated by proteinase K/SDS and RNase A digestion and organic extraction (12). For pulsed-field gel electrophoresis, cells were embedded in low-melting-point agarose at a concentration of 0.9×10^7 cells per ml, and DNA was prepared as described (13).

Inverse PCR. After restriction endonuclease digestion of 10 μg of genomic DNA, incompatible cohesive ends were filled in with Klenow polymerase. Fragments were diluted to 0.5 μg/ml and circularized with T4 DNA ligase (2 units/μl) in 50 mM Tris, pH 7.8/10 mM $MgCl_2$/0.05 mM ATP/20 mM dithiothreitol/0.005% bovine serum albumin at 16°C. The inverse PCR mixture contained template at 1 ng/μl, each dNTP at 0.2 mM, each oligonucleotide primer at 1 μM, $MgCl_2$ at 1.5 mM, standard buffer, and AmpliTaq polymerase (Perkin–Elmer/Cetus) at 25 milliunits/μl. Temperature cycling consisted of 30–40 cycles of 1 min of denaturation at 94°C, 1 min of annealing at 55°C, and 3 min of extension at 72°C in an automatic cycler (Coy Laboratory Products, Ann Arbor, MI).

The publication costs of this article were defrayed in part by page charge payment. This article must therefore be hereby marked "*advertisement*" in accordance with 18 U.S.C. §1734 solely to indicate this fact.

Abbreviation: TK, thymidine kinase.

‡To whom reprint requests should be addressed.
¶Present address: Children's Hospital, 8001 Frost Street, San Diego, CA 92123.

††The sequences reported in this paper have been deposited in the GenBank data base (accession nos. M80242 and M80243).

Subcloning and DNA Sequencing. PCR products were purified in Centricon microconcentrators (Amicon), digested at endonuclease sites engineered into the primers, electrophoresed in agarose gels in Tris/acetate buffer, and isolated by the glass-powder technique (14). Isolated fragments were ligated into the plasmid pBluescript SK (Stratagene). Competent *Escherichia coli* HB101 cells (BRL) were transformed with the ligation product. Double-stranded sequencing of plasmid inserts was performed with Sequenase version 2.0 (United States Biochemical). To check for sequence variations introduced during PCR amplification, two or three subclones were sequenced.

Electrophoresis and Southern Blot Analysis. For conventional electrophoresis, DNA samples were digested with 3–10 units of restriction endonuclease per μg of DNA for 2–6 hr and electrophoresed in 0.4–1.2% agarose gels in Tris/borate buffer. For pulsed-field gel electrophoresis, agarose gel slices containing 2–3 μg of embedded DNA were incubated overnight with 30 units of restriction endonuclease and the digested DNA was electrophoresed in 1% agarose gels in Tris/borate buffer with a CHEF-DR II apparatus (Bio-Rad). Genomic DNA electrophoresed in agarose gels was blotted to nylon membranes (GeneScreen*Plus*, NEN). Plasmid inserts were isolated by the glass-powder technique (14), labeled by the random-primer technique (15), and hybridized with the membranes.

Chromatin Analysis. RJK92 cells were labeled with [6-^{3}H]deoxycytidine as described (8). Following cell harvest, nuclei were isolated by lysis in 0.27% Nonidet P-40 and Dounce homogenization followed by sucrose step gradient centrifugation (16). Nuclei were digested with DNase I (Boehringer Mannheim), and the extent of digestion was determined as described (16).

RESULTS

Inverse PCR Analysis of Rearrangement in Line 15. Southern blot analysis of carcinogen-induced TK$^+$ line 15 has previously identified a rearrangement whose breakpoint lies in a 400-base-pair (bp) region 5.6 kilobases (kb) 5′ to the TK gene (8, 9) (Fig. 1). From the cloned 5′ region of the wild-type TK gene (8), we subcloned and sequenced the corresponding wild-type 400-bp *Xmn* I fragment and the adjacent 400-bp *Xmn* I–*Nco* I fragment (Figs. 1 and 2*A*). Divergent primers were designed from the sequence at the 3′ end of this region. To amplify the rearrangement breakpoint fragment from line 15, genomic DNA was cleaved with *Bam*HI and *Eco*RI to generate a 620-bp fragment that spans the rearrangement breakpoint (Fig. 1). This combination of endonucleases generates a small rearranged fragment and a larger wild-type fragment, which will not be efficiently amplified. Compatible blunt ends were next created by filling in the incompatible *Bam*HI and *Eco*RI ends with Klenow polymerase. Ligation was performed at low DNA concentrations to promote fragment circularization. Finally, the breakpoint fragment was amplified by PCR using the divergent primers from the 5′ TK region (Figs. 1 and 2*A*).

The resulting PCR product was isolated and subcloned into a plasmid. Sequence analysis demonstrated a novel region juxtaposed to the appropriate region of the TK gene (Fig. 2). A *Bam*HI–*Bgl* I restriction fragment from this novel region was isolated (Figs. 1 and 2*A*). Southern blot analysis with this probe demonstrated hybridization to a unique locus in RJK92 DNA and hybridization to a rearranged fragment in line 15 DNA that is identical to that detected by a 5′ TK probe (data not shown). These data indicate that the correct rearranged fragment was isolated.

Inverse PCR of Wild-Type RP15 Region. By using the probe for the rearrangement partner (referred to as RP15), a restriction map of the wild-type RP15 region was constructed

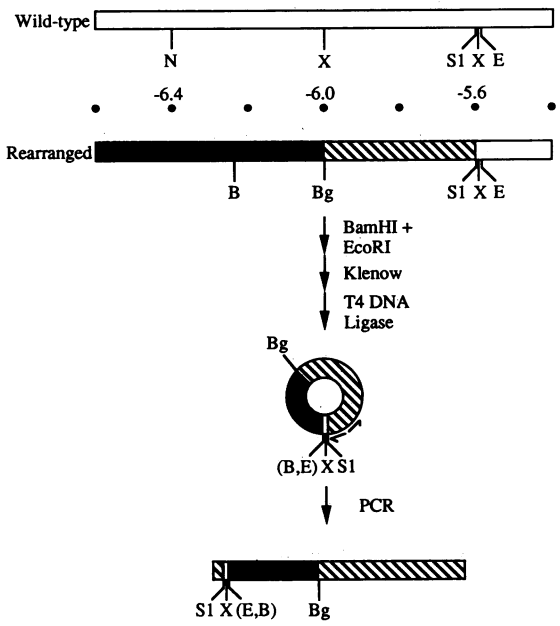

FIG. 1. Inverse PCR strategy for isolation of rearrangement breakpoints. The wild-type and rearranged copies of the 5′ TK region in line 15 (8) are shown. In the rearranged copy, the rearrangement partner is shaded and the breakpoint has been localized to the hatched region (8). The numerical scale represents distances (kb) from the origin of transcription of the TK gene. Restriction endonuclease abbreviations are listed in the legend to Fig. 3. The arrows around the circle represent the PCR primers (see Fig. 2). The ligated *Eco*RI and *Bam*HI sites are in parentheses.

by Southern blot analysis of RJK92 DNA (Fig. 3*A*). The map of the wild-type region 5′ to the breakpoint site is identical to the map of the region 5′ to the rearrangement breakpoint in line 15 (8), thus indicating that the rearrangement is a joining of two physically separated regions and not a more complex set of rearrangements. The wild-type RP15 region 3′ to the breakpoint site was then isolated by inverse PCR of unrearranged RJK92 DNA. As indicated by the map (Fig. 3*A*), a small junctional fragment was generated by digestion of RJK92 DNA with *Bam*HI and *Taq* I. After filling in of incompatible ends with Klenow polymerase and ligation at low DNA concentration, PCR with divergent primers from the known RP15 region generated a fragment of the expected size. This fragment was subcloned and sequenced to complete the wild-type RP15 sequence (Fig. 2*B*).

Sequence Comparison of the 5′ TK and RP15 Regions. The sequence of the rearranged fragment in line 15 was compared with the sequences of the wild-type 5′ TK and RP15 regions (Fig. 2*C*). The rearrangement consists of a precise fusion of RP15 and 5′ TK sequences without loss or addition of nucleotides. Directly at the breakpoint in each wild-type rearrangement partner, there is a 2-bp sequence, CpT, one copy of which is present in the rearranged fragment. There are also 4- to 5-bp blocks of sequence identity around the breakpoint, but these blocks are not precisely aligned and thus are of unknown significance. Therefore, there is minimal homology between the rearrangement partners near the breakpoint.

Comparison of the remainder of the sequenced regions of the two wild-type rearrangement partners also failed to reveal any regions with significant homology. One common structural feature is a 25-bp A+T-rich block located 38 or 65 bp 5′ to the breakpoint sites (Fig. 2 *A* and *B*). Otherwise, there are no significant stretches of homopurines, homopyrimidines, or alternating purines and pyrimidines. A highly repetitive element identified as a hamster type B1 *Alu* repeat is present

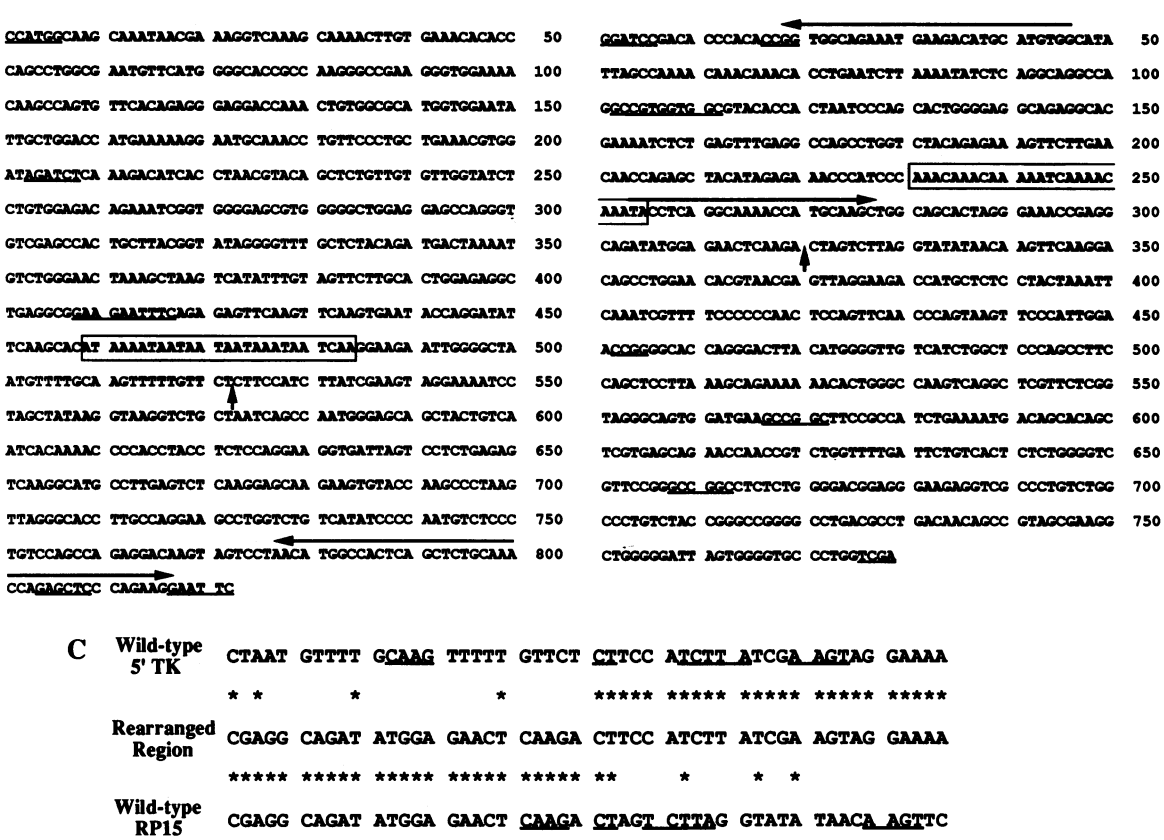

FIG. 2. (*A* and *B*) Sequences of wild-type 5′ TK and RP15 regions. Vertical arrows indicate the rearrangement breakpoints in line 15, and boxes enclose nearby A+T-rich regions. Pertinent restriction endonuclease sites are underlined and positions of inverse PCR primers are indicated by horizontal arrows. The sequences of the 5′ TK primers (with the restriction sites underlined) are TTCCTGCAGAGCTGAGTGGCCATGTT and AAACCAGAGCTCCCAGAAGG. The sequences of the RP15 primers are CCACATGGAGATCTTCATTTCTGCCACC and TACCTCGAGCAAAACCATGCAAGC. (*C*) Comparison of sequences of rearranged region with wild-type 5′ TK and RP15 regions. Correctly aligned nucleotides are indicated by stars, and blocks of sequence identity are underlined.

in the RP15 region 65–220 bp 5′ to the breakpoint site. No repetitive elements were identified by sequence or hybridization analysis of the corresponding 5′ TK region.

Long-Range Analysis of TK and RP15 Regions. Southern blot analysis of line 15 with a probe from the wild-type RP15 region 3′ to the breakpoint site demonstrated a wild-type band with a hybridization intensity less than that of the band in the parent RJK92 (data not shown). No rearranged bands were present, and therefore these results indicate that the RP15 region 3′ to the rearrangement breakpoint is deleted in line 15. In conjunction with the previous result that the TK region 5′ to the rearrangement breakpoint is also deleted in this line (8), these data suggest that the rearrangement in line 15 is a simple deletion between the RP15 and TK regions.

To test this hypothesis, we employed infrequently cutting restriction endonucleases and pulsed-field gel electrophoresis to search for a large restriction fragment that hybridizes to RP15 and TK probes. Sequential hybridization of Southern blots of RJK92 and V79 DNA digests with TK and RP15 probes demonstrated a 50-kb *Sfi* I band and a 75-kb *Bss*HII band that hybridize to each probe (Fig. 4). This result indicates that the RP15 and TK regions are colinear and separated by a maximum of 50 kb. Hybridization to different *Not* I fragments is consistent with the presence of a *Not* I site between the two sequences used as probes (Fig. 3*A*). The *Sfi* I sites were localized by Southern blot analysis, and the restriction maps of each region (8, 9) were combined to construct a long-range map of the wild-type TK-RP15 region (Fig. 3*B*). This map indicates that the rearrangement in line 15 consists of a 35-kb deletion between the RP15 and TK regions.

Methylation and Chromatin Analysis of RP15 Region. One of the important attributes of this inducible rearrangement system is the availability of a parental cell line that permits examination of the nuclear organization prior to the rearrangement event. Active genes are often located adjacent to 1- to 2-kb regions enriched for demethylated CpG dinucleotides (17). These CpG islands can be identified by the abundance of sites for infrequently cutting, methylation-sensitive restriction endonucleases. Using the *Bam*HI–*Bgl* I RP15 probe, we investigated the presence of demethylated CpG islands in the RP15 region. Hybridization of this probe to genomic DNA digested with the methylation-insensitive endonuclease *Bcl* I demonstrates a 6.5-kb band. Double digestion with *Bcl* I and one of a group of methylation-sensitive restriction enzymes generated smaller bands, ranging in size from 3.0 to 4.1 kb (Fig. 5*A*). This result indicates that there is a demethylated CpG island between map positions 0 and +2 kb (Fig. 3*A*). Further analysis revealed a small cluster of partially or fully methylated CpG sites between map positions −3.5 and −4.0 kb (Fig. 3*A*) and a demethylated CpG island 30 kb 5′ to the RP15 island (Fig. 3*B*).

Other investigators have demonstrated that DNase I cleaves chromatin regions in which the nucleosomal array is disrupted by other DNA-binding proteins (18). We analyzed the RP15 region for altered chromatin structure by digestion of RJK92 nuclei with various amounts of DNase I, followed by DNA isolation, digestion with *Kpn* I, *Eco*RV, or *Bcl* I, and Southern blot analysis with the *Bam*HI–*Bgl* I probe (Fig. 5*B*). Two major and at least three minor DNase I-hypersensitive sites were detected in the RP15 region. Two of the hyper-

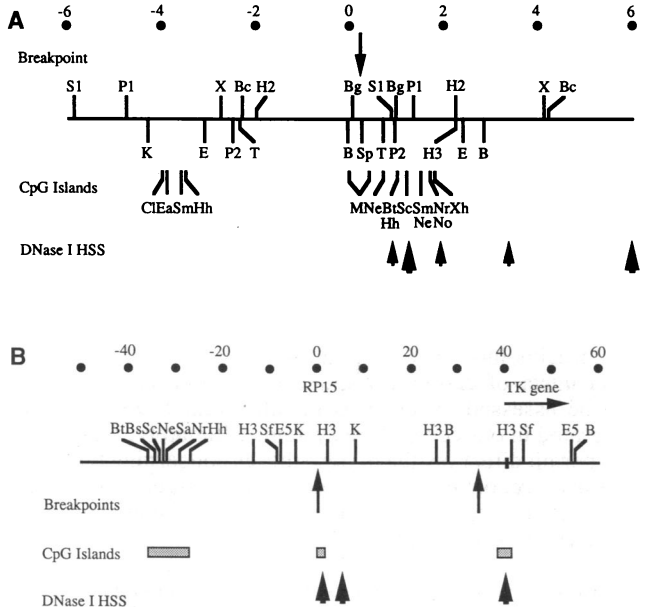

FIG. 3. Map of the wild-type RP15 region (*A*) and long-range map of the wild-type RP15 and TK regions (*B*). Locations of rearrangement breakpoints in line 15 are shown by vertical arrows. Sites for methylation-insensitive restriction endonucleases are presented in the top section of each map. CpG islands are shown in the middle section of each map as clustered methylation-sensitive endonuclease sites or shaded boxes. Major and minor DNase I-hypersensitive sites (HSS, indicated by large and small arrowheads, respectively) are indicated in the bottom section of each map. [The demethylated CpG island and HSS in the 5′ TK region appear following gene activation (8, 9)]. In *B*, the first exon of the TK gene and direction of transcription are shown as a vertical bar and horizontal arrow, respectively. The numerical scale represents distances (kb) from an arbitrary point. Restriction enzymes: B, *Bam*HI; Bc, *Bcl* I; Bg, *Bgl* I; Bs, *Bss*HII; Bt, *Bst*UI; Cl, *Cla* I; E, *Eco*RI; E5, *Eco*RV; Ea, *Eag* I; H2, *Hin*cII; H3, *Hin*dIII; Hh, *Hha* I; K, *Kpn* I; M, *Msp* I/*Hpa* II; N, *Nco* I; Ne, *Nae* I; No, *Not* I; Nr, *Nar* I; P1, *Pst* I; P2, *Pvu* II; S1, *Sac* I; Sa, *Sal* I; Sc, *Sac* II; Sf, *Sfi* I; Sm, *Sma* I/*Xma* I; Sp, *Spe* I; T, *Taq* I; X, *Xmn* I; Xh, *Xho* I.

sensitive sites map within the CpG island around map position +1 kb and three sites map 3′ to this region (Fig. 3*A*).

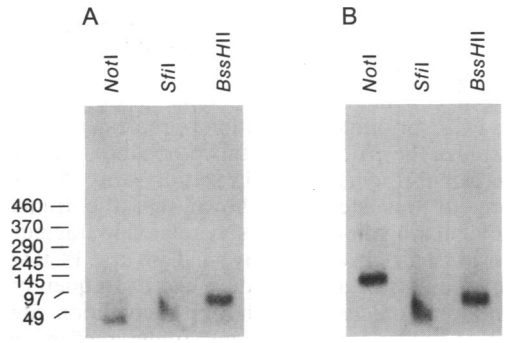

FIG. 4. Long-range analysis of RP15–TK region. Hamster V79 DNA samples were digested with the designated enzymes and fractionated by pulsed-field gel electrophoresis in a 1% agarose gel. The blot was hybridized to the 400-bp *Xmn* I fragment from the 5′ TK region (*A*) and the 100-bp *Bam*HI–*Bgl* I fragment from the RP15 region (*B*). Representative sizes (kb) of *Saccharomyces cerevisiae* chromosomes and concatemerized λ DNA marker fragments are shown at left.

Southern blot analysis of the *Eco*RV digest permitted examination up into the TK region and did not detect any hypersensitive sites 3′ to the site at map position +5.7 kb. This result agrees with the previously demonstrated absence of DNase I-hypersensitive sites in TK genes of TK⁻ RJK92 cells and appearance of these sites after TK gene activation (8).

DISCUSSION

To identify structural features relevant to the mechanism of genomic rearrangement, we analyzed a hamster cell culture system in which rearrangements are induced at the endogenous TK locus by chemical carcinogen treatment (8, 9). The rearrangement breakpoint and wild-type regions involved by one such rearrangement (line 15) were isolated by an inverse PCR approach. Sequence analysis of the 5′ TK region and its rearrangement partner RP15 demonstrated a 2-bp direct repeat at the breakpoint sites and 25-bp A+T-rich blocks located ≈55 bp 5′ to each breakpoint. Methylation and chromatin analysis of the wild-type RP15 region revealed a demethylated CpG island and a complex of DNase I-hypersensitive sites situated adjacent to the site of the rearrangement breakpoint. These active chromatin elements are elim-

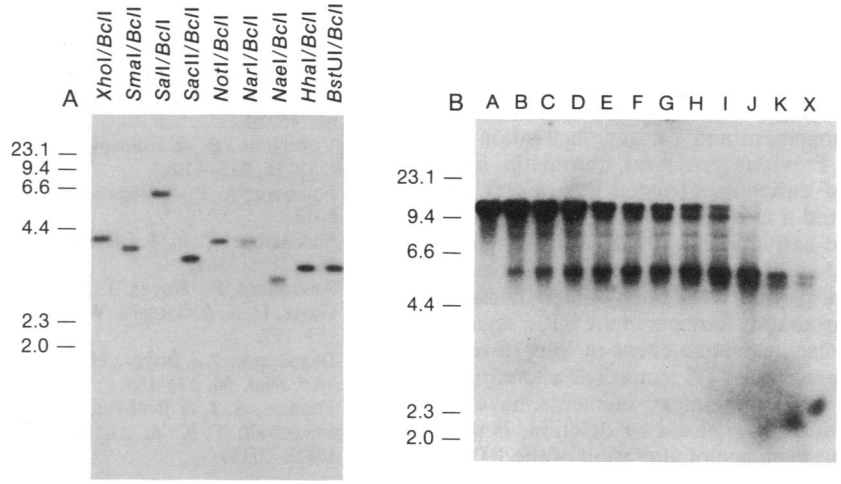

FIG. 5. Methylation (*A*) and chromatin analysis (*B*) of RP15 region. (*A*) RJK92 DNA samples were digested with the designated enzymes, electrophoresed in a 1.2% agarose gel, and blotted. (*B*) After digestion of RJK92 nuclei with increasing concentrations of DNase I, DNA was isolated, digested with *Kpn* I, electrophoresed in a 0.75% agarose gel, and blotted. Blots from *A* and *B* were hybridized to the 100-bp *Bam*HI–*Bgl* I fragment from the RP15 region. Sizes (kb) of *Hin*dIII fragments of λ DNA are shown at left. Extents of DNase I digestion (percentage soluble in perchloric acid): lane A, 0%; lane B, 0.1%; lane C, 0.2%; lane D, 0.3%; lane E, 0.3%; lane F, 0.3%; lane G, 0.4%; lane H, 0.5%; lane I, 0.6%; lane J, 0.8%; lane K, 1.8%; lane X, 1.9%.

inated by the rearrangement in line 15, which consists of a 35-kb deletion between the 5′ TK and RP15 regions.

As an alternative to genomic library preparation for each rearranged cell line, we have demonstrated the utility of inverse PCR for efficient isolation of rearranged sequences. To maximize the efficiency of this procedure, we focused on the junctional-fragment circularization step. Mathematical modeling of this step has shown that the frequency of intramolecular ligation is inversely related to fragment length (19). To construct an adequately small inverse PCR template, we employed strategies including use of frequently cutting restriction endonucleases with 4-bp recognition sites, combination of two endonucleases and filling in of incompatible ends with Klenow polymerase, and ligation of blunt ends. Using these strategies, we have been successful when the inverse PCR template size is <1 kb.

Sequence analysis of carcinogen-induced rearrangements has indicated similarities to tumor-associated rearrangements. As observed in deletions of the *RB1* gene in retinoblastoma (3), there are only very short blocks of homology at the breakpoints in the wild-type rearrangement partners. This minimal homology may be related to the choice of the exact breakpoint site by a mispairing process. However, the absence of more substantial sequence similarity between the partners indicates an overall nonhomologous recombination mechanism. The presence of A+T-rich sequences near the breakpoints in the wild-type TK and RP15 regions is reminiscent of cases of *BCR–ABL* rearrangement in leukemias (4). The relative ease of denaturation of A+T-rich regions may permit adoption of a non-B-DNA conformation. This altered structure may bind specific factors and serve to facilitate the accessibility of the region for recombination.

We have also investigated the utility of this inducible cell culture system for analysis of the nuclear organization of the rearrangement partners in the parental cell type. Our findings of a demethylated CpG island and an active chromatin complex directly adjacent to the rearrangement breakpoint site in the wild-type RP15 region indicate the presence of an active gene in this region (17). The proximity of these active chromatin elements to the rearrangement breakpoint suggests that they may function in the rearrangement process. A relationship between transcriptional activity and recombination has been suggested from investigations of recombination in yeast (20) and V(D)J rearrangement of the immunoglobulin and T-cell receptor loci (21). These findings are compatible with hypotheses that the altered chromatin structure of transcriptionally active loci is more accessible to the recombination machinery or that factors necessary for recombination are associated with these active loci or the transcription process.

Our findings can be interpreted with respect to the relationship between rearrangement and TK gene activation in our cell culture system. Previous structural, chromatin, and methylation analyses of carcinogen-treated derivatives of RJK92 have demonstrated a close association between TK gene rearrangement and activation (8, 9). However, these studies failed to reveal evidence of regulatory elements introduced into the vicinity of the TK gene by the rearrangements (8). The active chromatin elements in the RP15 region are eliminated by the rearrangement event in line 15 and therefore are not juxtaposed to the TK locus. The alternative hypothesis, that these RP15 regulatory elements have a suppressive influence which is released by deletion, is unlikely because there is no evidence of alteration of the RP15 region in other TK^+ derivatives of RJK92 (data not shown). We therefore propose that rearrangements follow and are facilitated by activation of the carcinogen-damaged TK locus. In this scenario, an active chromatin domain and demethylated CpG island would be present at the TK and RP15 loci at the time of rearrangement. As illustrated in Fig. 3*B*, there is a similarity between the positions of the breakpoints and active chromatin elements in the TK and RP15 loci. This symmetrical relationship suggests that these elements may function to direct the recombination machinery to the ends of the rearrangement.

Our analysis of the regions involved in one rearrangement event has revealed the sequence and chromatin features near the breakpoints. The generality of these features in the mechanism of carcinogen-induced genomic rearrangement can be assessed by analysis of other rearranged cell lines generated in our cell culture system. Ultimately, this system will permit direct testing of hypotheses concerning the mechanism of genomic rearrangement by manipulating components of the inducible system and determining the consequences of each manipulation.

This work was supported in part by funds from Grant CA47983 from the National Cancer Institute and Postdoctoral Training Grant 5-T32-GM-08252 (to F.G.B.) from the National Institutes of Health.

1. Tycko, B. & Sklar, J. (1990) *Cancer Cells* **2**, 1–8.
2. Chen, S. J., Chen, Z., Font, M. P., d'Auriol, L., Larsen, C. J. & Berger, R. (1989) *Nucleic Acids Res.* **17**, 7631–7642.
3. Canning, S. & Dryja, T. P. (1989) *Proc. Natl. Acad. Sci. USA* **86**, 5044–5048.
4. Papadopoulos, P. C., Greenstein, A. M., Gaffney, R., Westbrook, C. A. & Wiedemann, L. M. (1990) *Genes Chromosomes Cancer* **1**, 233–239.
5. Weinreb, A., Collier, D. A., Birshtein, B. K. & Wells, R. D. (1990) *J. Biol. Chem.* **265**, 1352–1359.
6. Boehm, T., Mengle-Gaw, L., Kees, U. R., Spurr, N., Lavenir, I., Forster, A. & Rabbitts, T. H. (1989) *EMBO J.* **8**, 2621–2631.
7. Sperry, A. O., Blasquez, V. C. & Garrard, W. T. (1989) *Proc. Natl. Acad. Sci. USA* **86**, 5497–5501.
8. Barr, F. G., Rajagopalan, S. & Lieberman, M. W. (1990) *Nucleic Acids Res.* **18**, 129–135.
9. Barr, F. G., Rajagopalan, S., MacArthur, C. A. & Lieberman, M. W. (1986) *Mol. Cell. Biol.* **6**, 3023–3033.
10. Ochman, H., Gerber, A. S. & Hartl, D. L. (1988) *Genetics* **120**, 621–623.
11. Triglia, T., Peterson, M. G. & Kemp, D. J. (1988) *Nucleic Acids Res.* **16**, 8186.
12. Barr, F. G., Kastan, M. B. & Lieberman, M. W. (1985) *Biochemistry* **24**, 1424–1428.
13. Smith, C. L., Warburton, P. E., Gaal, A. & Cantor, C. R. (1986) in *Genetic Engineering: Principles and Methods*, eds. Setlow, J. K. & Hollaender, A. (Plenum, New York), Vol. 8, pp. 45–70.
14. Vogelstein, B. & Gillespie, D. (1979) *Proc. Natl. Acad. Sci. USA* **76**, 615–619.
15. Feinberg, A. P. & Vogelstein, B. (1983) *Anal. Biochem.* **132**, 6–13.
16. MacArthur, C. A. & Lieberman, M. W. (1987) *J. Biol. Chem.* **262**, 2161–2165.
17. Antequera, F., Boyes, J. & Bird, A. (1990) *Cell* **62**, 503–514.
18. Gross, D. S. & Garrard, W. T. (1988) *Annu. Rev. Biochem.* **57**, 159–197.
19. Dugaiczyk, A., Boyer, H. W. & Goodman, H. M. (1975) *J. Mol. Biol.* **96**, 171–184.
20. Thomas, B. J. & Rothstein, R. (1989) *Cell* **56**, 619–630.
21. Blackwell, T. K. & Alt, F. W. (1989) *J. Biol. Chem.* **264**, 10327–10330.